Acta Technica 62 No. 4B/2017, 1–16

Vertical mechanical-electric coupling vibration analysis of in-wheel motor electric vehicle[1]

Shi Peicheng[2,4], Peng Shanshan[3,5], Zhao Xuesong[2,6], Xiao Ping[2,7], Zhang Rongyun[2,8], Wang Xuejiao[2,9], Nie Gaofa[2,10]

Abstract. To study the influence of in-wheel motor on the running performance of electric vehicle and explore the design theory and vibration suppression method of wheel hub driving system, this research is carried out in the following procedures. First, a vertical kinetic model of 1/4 vehicle is built. Then a vertical mechanical-electric coupling vibration simulation model of in-wheel-motor electric vehicle composed of vertical kinetic model, torque ripple model of motor, random road model is established. Second, an in-wheel motor test system is established to verify the simulation results of motor torque ripple. Third, a mechanical-electric coupling vibration simulation model influenced by the torque ripple of motor is built through MATLAB/SIMULINK. Through this model, this paper analyses the vibration of vehicle and wheel so as to find the vertical mechanical-electric coupling vibration performance of in-wheel-motor electric vehicle. The results show that there is an obvious fluctuation in the speed and torque of motor after the motor is applied with load. As the load rises, the fluctuation quantity of speed and torque both increase. Besides, the torque ripple of motor exerts a large influence on the vertical vibration of the suspension system of vehicle, especially the wheel (unsprung mass). In consequence, the grip of tire is weakened, which is detrimental to the running safety of vehicle. The research results can provide theories and

[1]The authors would like to thank the financial supports of the National Natural Science Foundation of China (Grant No. 51575001), of Anhui province science and technology research key project (Grant No. 1604a0902158), of Anhui university scientific research platform innovation team building projects (2016-2018), and of Anhui Polytechnic University Young and middle-aged top-notch talent project (2016BJRC010).

[2]Anhui Polytechnic University, Anhui Engineering Technology Research Center of Automotive New technique, Wuhu 241000

[3]Anhui Institute of information Technology, Department of Mechanical Engineering, Wuhu 241100

[4]e-mail: shipeicheng@126.com

[5]e-mail: 1285096601@qq.com

[6]e-mail: 405833136@qq.com

[7]e-mail: 405833136@qq.com

[8]e-mail: 1815734402@qq.com

[9]e-mail: 1252973054@qq.com

[10]e-mail: 1151842608@qq.com

methods for the industrialized development of in-wheel motor electric vehicle and alternatives for the studies on the NVH performance of in-wheel motor electric vehicle.

Key words. Electric vehicle, in-wheel motor, suspension, vibration, coupling..

1. Introduction

In recent years, in-wheel-motor electric vehicle (driven by two or four electric wheels) has drawn much attention from the automobile industry both home and abroad for its unique advantages in compact structure and efficiency of power transmission [1], [2]. However, there are some controversial problems of in-wheel motor in practical engineering [3], [4]. First, the combination of motor and hub will increase the unsprung mass of vehicle, which adversely affects the vehicle's riding performance. Second, the motor is easily impacted by road as it is directly fixed on wheel, which may intensify the magnetic gap fluctuation between stator and rotor as well as reduce the service life of motor. Third, the torque ripple of motor affects wheel directly, which will lead to the sympathetic vibration of the front and back of suspension and the vibration of the whole drive system.

To find the impact of in-wheel motor on the driving performance of electric vehicle and study the design theory and vibration suspension method of wheel hub driving system, this paper, based on the magnetic moment analysis of motor, analyzes the vertical kinetic characteristics of in-wheel-motor electric vehicle and the mechanical-electric coupling vibration characteristics. Taking low-speed outer rotor in-wheel-motor electric vehicle as the object of study, this paper builds a 1/4 vehicle suspension model of in-wheel-motor electric vehicle and conducts a simulation test in MATLAB/SIMULINK using motor torque ripple model and random road model. Though the simulation test, this paper analyzes the effect of in-wheel motor torque ripple on the vertical vibration characteristics of vehicle and obtains the characteristic curves of vehicle's vertical vibration influenced or uninfluenced by the torque ripple of motor. This research purpose of this paper is to provide a theoretical basis for the researches on the vibration performance of in-wheel-motor electric vehicle as well as the service life and reliability of in-wheel system and the grip of tire.

2. Vertical kinetic model of in-wheel- motor electric vehicle

The kinetic model of in-wheel-motor electric vehicle is composed of suspension system and in-wheel motor system [5], [6]. The simplified vertical vibration model of 1/4 vehicle with in-wheel motor is shown in Fig. 1. In the vibration model, the motor mass and wheel mass are considered as two different parts. The electromagnetic torque ripple of motor is first transformed into exciting force, and then coupled into the vertical vibration model of 1/4 vehicle in the form of load. In this way, the influence of in-wheel motor on the vertical vibration of vehicle can be effectively analyzed.

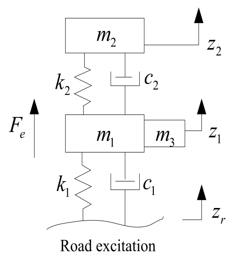

Fig. 1. 1/4 vehicle vertical vibration model of in-wheel-motor

According to Fig. 1, the vertical vibration kinetic equation of vehicle is

$$(m_1 + m_3)\,\ddot{z}_1 + c_1\,(\dot{z}_1 - \dot{z}_\mathrm{r}) + c_2\,(\dot{z}_1 - \dot{z}_2) + k_1\,(z_1 - z_\mathrm{r}) + k_2\,(z_1 - z_2) + F_\mathrm{e} = 0\,, \quad (1)$$

$$m_2\ddot{z}_2 + c_2\,(\dot{z}_2 - \dot{z}_1) + k_2\,(z_2 - z_1) = 0\,, \quad (2)$$

$$F_\mathrm{t} = k_1\,(z_1 - z_\mathrm{r}) + c_1\,(\dot{z}_1 - \dot{z}_\mathrm{r})\ , \quad (3)$$

$$F_\mathrm{n} = k_2\,(z_1 - z_2) + c_2\,(\dot{z}_1 - \dot{z}_2)\ , \quad (4)$$

$$F_\mathrm{e} = \frac{T_\mathrm{e}}{r}\,. \quad (5)$$

Where m_1 is unsprung mass (excludes the mass of in-wheel motor), m_2 is sprung mass; m_3 is the mass of in-wheel motor, k_1 and c_1 respectively are the stiffness and damping of tire, k_2 and c_2 respectively are the stiffness and damping of suspension, z_r, z_1 and z_2 are road roughness, wheel displacement, and vehicle displacement respectively, F_t is the grip of tire, F_n is the vibration input of sprung mass, F_e is the torque ripple input of in-wheel motor, T_e is the torque ripple input of motor, and r is the radius of vehicle wheel.

3. Modeling of road

A random excitation time-domain road model is built using white noise filtration method. The mathematical description of the model is

$$\dot{q}(t) + \alpha u q(t) = w(t)\,, \quad (6)$$

where $q(t)$ is random road excitation, α is constant, u is the speed of vehicle, and $w(t)$ is White Gaussian Noise.

The road can be divided into 8 classes, among which Class-B road is the closer to real read. Thus, based on equation (6), a Class-B simulation road is built through SIMULINK. The details of the simulation road are given later. The speed of vehicle is set at 30 m/s and the simulation time is 30 s. The curve of random road excitation is shown in Fig. 2.

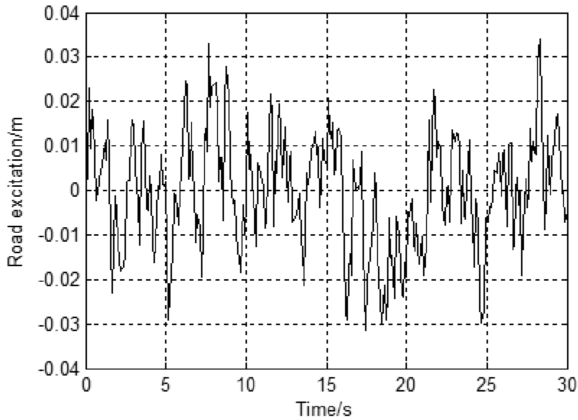

Fig. 2. The curve of Class-B Road excitation electric vehicle (speed of vehicle: 30 m/s)

4. Kinetic model of in-wheel motor torque ripple

4.1. Modeling of motor torque

The in-wheel motor adopted in this paper is a 10 kW PMSM. The speed of vehicle is set at 30 m/s. Then there are

$$n = \frac{30}{\pi d} \times 60 \approx 955\,\mathrm{rpm}\,, \tag{7}$$

$$P_{\mathrm{e}} = \frac{T_{\mathrm{e}} \cdot n}{9550} \Rightarrow T_{\mathrm{e}} = 100\,\mathrm{Nm}\,, \tag{8}$$

where d, the diameter of tire, is 600 mm.

The motor speed n and the output torque T_{e} can be obtained through expressions (7) and (8). The PMSM used in this paper has a rated power of 10 kW and a rated speed of 955 rpm. When the speed of vehicle is 30 m/s, the output torque T_{e} of motor is 100 Nm. It indicates that the PMSM is able to meet the vehicle's requirement on drive (four-wheel-hub drive or two-wheel-hub drive).

According to the motor theory, under ideal conditions and when the rotational speed of d/q axis and rotor are the same, the current model of PMSM can be obtained by using a d/q coordinate system, in which the speed of motor accords with the input current frequency of PMSM. The current model of PMSM is

$$\left\{ \begin{array}{l} \frac{\mathrm{d}}{\mathrm{d}t} i_{\mathrm{d}} = \frac{1}{L_{\mathrm{d}}} u_{\mathrm{d}} - \frac{R}{L_{\mathrm{d}}} i_{\mathrm{d}} + \frac{L_{\mathrm{q}}}{L_{\mathrm{d}}} p \omega_{\mathrm{r}} i_{\mathrm{q}} \\ \frac{\mathrm{d}}{\mathrm{d}t} i_{\mathrm{q}} = \frac{1}{L_{\mathrm{q}}} u_{\mathrm{q}} - \frac{R}{L_{\mathrm{q}}} i_{\mathrm{q}} + \frac{L_{\mathrm{d}}}{L_{\mathrm{q}}} p \omega_{\mathrm{r}} i_{\mathrm{d}} - \frac{\lambda p \omega_{\mathrm{r}}}{L_{\mathrm{q}}} \end{array} \right. . \tag{9}$$

Substitute expression (9) into the electromagnetic torque equation

$$T_{\mathrm{e}} = \frac{3}{2} p \left[\lambda i_{\mathrm{q}} + \left(L_{\mathrm{d}} - L_{\mathrm{q}} \right) i_{\mathrm{d}} i_{\mathrm{q}} \right] . \tag{10}$$

We get the kinematic equation of system

$$\frac{\mathrm{d}\omega_{\mathrm{r}}}{\mathrm{d}t} = \frac{1}{J} \left(T_{\mathrm{e}} - T_{\mathrm{m}} - F\omega_{\mathrm{r}} \right) , \tag{11}$$

$$\frac{\mathrm{d}\theta}{\mathrm{d}t} = \omega_{\mathrm{r}} . \tag{12}$$

Where L_{d} and L_{q} are the inductance of axes d and q, u_{d} and u_{q} are the voltage of axes d and q, R is the resistance of stator winding, i_{d} and i_{q} are the current of axes d and q, p is the number of pore-pairs, ω_{r} is the angular velocity of rotor, λ is linkage, T_{e} is electromagnetism, θ is the angular position of rotor, T_{m} is the torque of mechanical axis, F is viscous friction, and J is the moment of inertia.

4.2. Simulink modeling and simulation of motor

According to the vector control principle of PMSM, double closed loop control is used in the in-wheel motor system. The simulation model of the system (see Fig. 3) is built through Simulink. The system contains such modules as speed regulator, filter, and motor measure. The values of parameters are listed in Table 1.

Table 1. The value of motor parameter

Motor parameter	Value
L_{d}, L_{q} (H)	0.026
R (Ω)	2.4
u_{d}, u_{q} (V)	0.167
J (kgm^2)	0.0008
P	4
λ (W$_{\mathrm{s}}$)	0.143
P_{e} (kW)	10
n (rpm)	955
F	0

Through step, the system is able to apply a step load of 100Nm to the motor 1.5 seconds later. The simulation time is 5 seconds. Then we get the output response of motor (see Figs. 4 $\sim$ 6).

As is shown in Fig. 4 (simulation curve), the no-load torque of motor between 0 and 1.5 s fluctuates around 0. The motor torque will quickly rise and reach the target value 100 Nm 1.5 s later. After a short time of jumping, the value of torque

Table 2. Parameters of the vertical vibration model of 1/4 vehicle

Vehicle parameter	Initial value
Unsprung mass m_1 (kg)	25
Sprung mass m_2 (kg)	200
In-wheel motor mass m_3 (kg)	20
Stiffness of tire k_1 (N/m)	190000
Damping of tire c_1 (N/(m/s))	400
Stiffness of suspension k_2 (N/m)	18000
Damping of suspension c_2 (N/(m/s))	1600
Radius of wheel r (m)	0.3

stabilizes and fluctuates around 100 Nm. The fluctuation may be caused by the interaction between the stator field and the rotor field, namely, harmonic torque.

As is shown in Fig. 5 (simulation curve), the motor speed zooms when the motor starts, indicating a quick response. The motor reaches the target speed 100 rad/s in 0.5 s and then runs steady. The motor speed changes rapidly when the motor is applied with a sudden load at 1.5 s (the load torque is 100 Nm) and becomes stable soon. Only a slight fluctuation can be observed in the motor speed after the motor becomes stable. It indicates that the proposed PMSM model has a good performance in speed control and speed stabilization.

The dynamic mechanical characteristics of motor is shown in Fig. 6, where A refers to the working point when the no-load speed reaches the reference speed and B refers to the working point when the motor is influenced by load torque. The working point transfers from A to B after the motor is applied with load. As is shown in Fig. 6, the motor speed slightly declines at first and then bounces back to the target value in a short time.

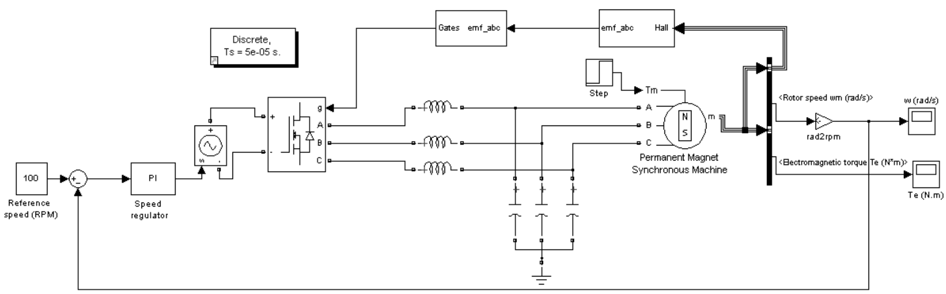

Fig. 3. Simulink model of motor

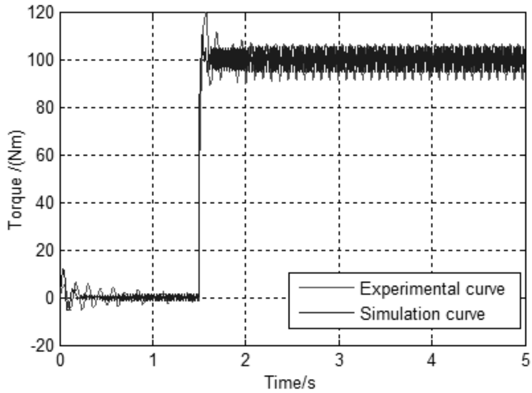

Fig. 4. Response of motor torque output

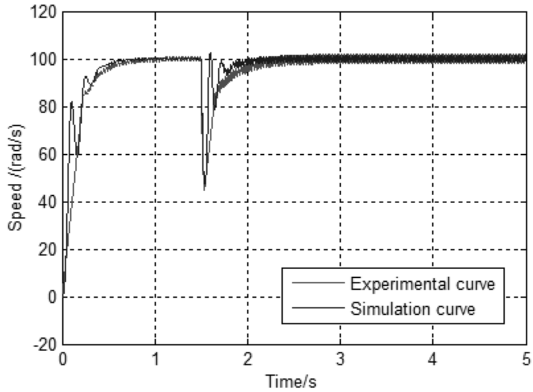

Fig. 5. Response of motor speed output

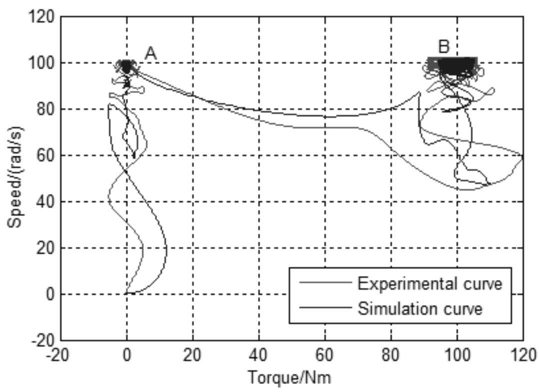

Fig. 6. Curves of motor mechanical characteristic

5. Experimental verification

To verify the response of motor speed output and the simulation results of torque ripple, an in-wheel motor test system was built (see Fig. 7).

In the test, the magnetic powder brake is used as simulation loader which can control the loading torque. The motor speed & torque sensor monitors the fluctuation in speed and torque in real time. Three-jaw chuck is used to clamp the stator axle of motor. The motor is an external rotor electric machine.

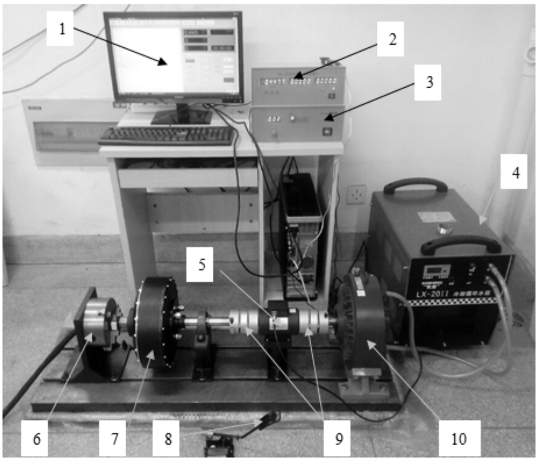

Fig. 7. Motor test bench. 1- PC; 2- Rotational speed & torque collecting instrument; 3- Load controller; 4- Circulating cooling water tank; 5- Motor speed & torque sensor; 6- Three jaw chuck; 7- Permanent magnet synchronous motor; 8- Motor speed control pedal; 9- Double diaphragm coupling; 10- Magnetic powder brake.

The proposed motor test system is a closed-loop control system, in which the motor speed & torque sensor is used to monitor and measure the speed and torque of motor in real time. The measured data is transferred to the host computer through RS485 serial port. The host computer will process the data and then issue instructions to the load controller. Thus, the load controller can adjust the simulated load torque. All instruments in the test system are connected with the PC through RS485 bus for the automatic loading of motor and the centralized collection of data.

A PMSM with a nominal voltage of 72 V and a raged power of 10 kW is tested though the motor test bench. Assisted by the motor speed control pedal, the motor is able to start under the conditions of zero-load. In other words, no load is applied on the magnetic powder brake. To compare the test curves with the abovementioned simulation curves, the target speed is set at 955 rpm (100 rad/s). The load torque reaches 100 Nm instantly when the motor is applied with load by the load controller at 1.5 s. The test results are shown in Figs. 4$\sim$6.

As is shown in Fig. 4 (experimental curves), the motor speed rises rabidly when it starts, which indicates a quick response. The motor reaches the target speed 100 rad/s in 0.6 s and then keeps running steadily. When the motor is applied with a sudden load at 1.5 s, the load torque zooms to 100 Nm, in which case, the motor speed declines rabidly and then becomes steady again in 0.6 seconds. After the motor resumes steady running, the motor speed fluctuates more greatly. The fluctuation value is about 2 %.

It can be known from Fig. 5 that the unloaded torque of motor between 0 and 1.5 s fluctuates around 2 Nm. It should be pointed out that the torque is caused by the axle friction and inertia moment of such machine elements as magnetic powder brake. When the motor is applied with a sudden load at 1.5 s, the load torque zooms to the target value 100 Nm, indicating a quick response motor torque. Then the load torque becomes steady after 0.5 seconds of jumping and keeps fluctuating around the target value. The fluctuation value is about 10 %.

As is shown in Fig. 6, there is an obvious fluctuation in the speed and torque of motor while the working point A transfers to working point B. However, both the speed ripple and torque ripple are convergent and are able to go back to the target value.

It can be observed from Figs. 4∼6 that the variation trends of experimental results and simulation results are in accordance with each other. Therefore, conclusions can be drawn that the proposed simulation model of motor is accurate and reliable, and can fully reflect the working situations of real motor. The fluctuations in the torque and speed of motor are both slight when the motor works without extra load. However, an obvious fluctuation can be observed in the torque and speed of motor after it is applied with a sudden load. The fluctuation values of torque and speed are about 10 % and 3 % respectively. The fluctuation values of simulation curves are slightly lower than those of experimental curves due to the simplification of model which has ignored some environmental influences.

According to the above analyses, the torque ripple of motor is real and will be magnified as the load increases. As for the specific influence of the torque ripple of motor on the vertical vibration of vehicle, further studies based on whole vehicle model are needed.

6. The mechanical-electric coupling vibration simulation under motor torque ripple

6.1. Modeling of the vertical vibration of 1/4 vehicle

As there no reduction gears in the outer-rotor in-wheel motor, the torque ripple produced by the motor will directly act on the hub and wheel. According to expressions (1) – (5), the simulation model established through MATLAB/SIMULINK is shown in Fig. 8. The model consists a 1/4 vehicle vertical vibration module, a road excitation module, and an in-wheel motor. The parameter values of the model are listed in Table 2.

6.2. Simulation analysis

A PMSM whose mass is 20 kg, nominal power is 10 kW, and rated speed is 955 rpm is used in the vibration simulation model shown in Fig. 8. The fluctuation value (simulation curves) when the output torque of motor is 100 Nm (see Fig. 4) and the Class-B road random excitation when the speed of vehicle is 30 m/s (see Fig. 2) are both vibration input. The simulation object is a vertical mechanical-electric coupling kinetic model of 1/4 vehicle (see Fig. 1).

The simulation time is 5 s. To find influence of in-wheel motor on the vertical mechanical-electric coupling vibration of suspension, simulation analysis was carried out on such variables as the vibration input F_{n} of sprung mass m_2, the dynamic load F_{t} of wheel, the vertical vibration acceleration of wheel ($\ddot{z}_1$) and vehicle ($\ddot{z}_2$), the vertical dumping speed of wheel ($\dot{z}_1$) and vehicle ($\dot{z}_2$), and the vertical displacement of wheel (z_1) and vehicle (z_2). The simulation results are shown in Figs. 9∼16, where the "non-torque ripple" refers to the fluctuation when the motor mass m_3 is included in the unsprung mass and the road is the main vibration source. The "torque ripple" refers to the fluctuation when the motor mass m_3 is included in the unsprung mass, and the exciting force F_{e} transformed from the torque ripple of motor is included in road excitation, and the exciting force F_{e} of motor and the random road are both vibration sources. In other words, the exciting force F_{e} of motor and random road excitation act on the vertical vibration model of 1/4 vehicle shown in Fig. 8 simultaneously.

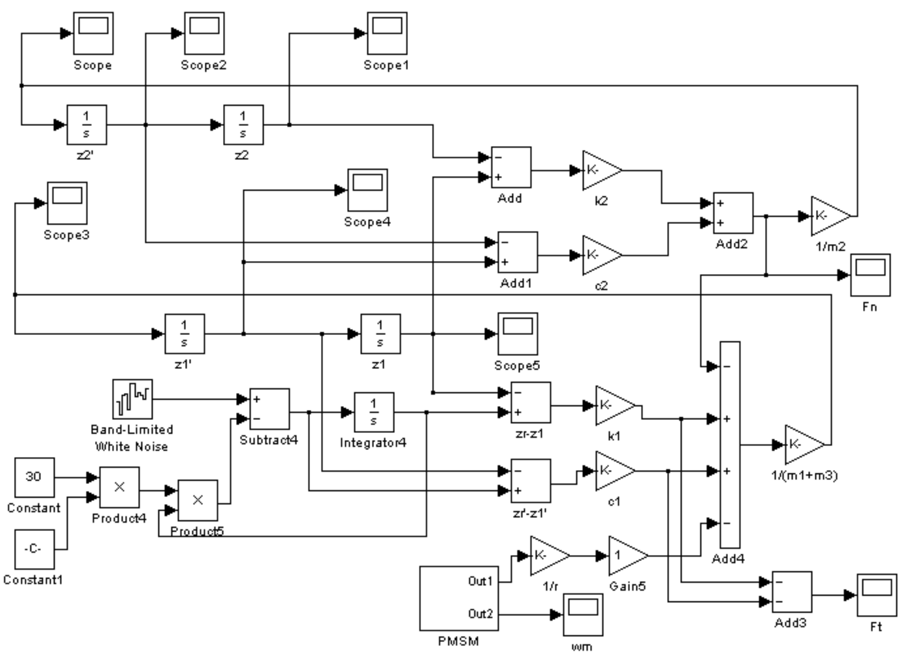

Fig. 8. The vertical vibration Simulink model of 1/4 vehicle

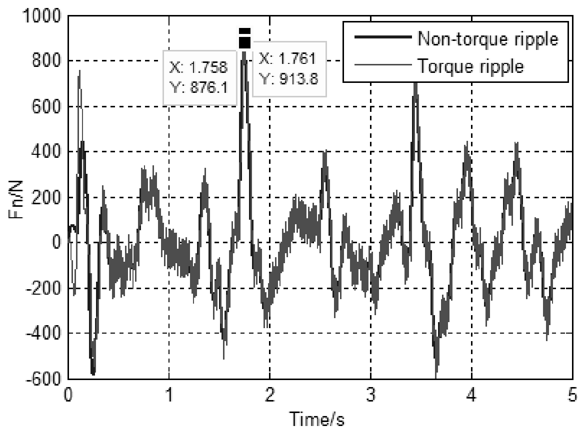

Fig. 9. Response of the vibration input F_{n} of sprung mass m_2

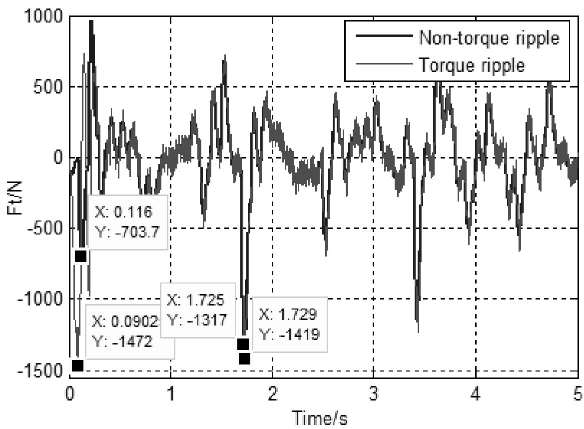

Fig. 10. Response of the dynamic load F_{t} of wheel

6.3. Analysis of results

As is shown in Figs. 9∼16, when the motor mass is 20 kg and the output electromagnetic torque is 100 Nm, the torque ripple of motor exerts an influence on the amplitude of all testing parameters of the suspension vibration system. Figures 9 and 10 respectively show the simulation curves of the vibration input F_{n} of sprung mass m_2 and the fluctuation value of tire grip F_{t}. It can be observed from Figs. 9 and 10 that the torque ripple of motor has a great influence on the tire grip F_{t}. The peak growth rate of tire grip around 0.1 s is about 54 %. The tire grip changes within a certain range as the torque ripple of motor becomes stable. The growth rate of tire grip around 1.7 s is about 7.6 %. The changing rate of the vibration F_{n} of sprung mass m_2 is lower than that of tire grip. As the torque ripple becomes stable, the growth rate of the vibration F_{n} of sprung mass m_2 around 1.7 s is only

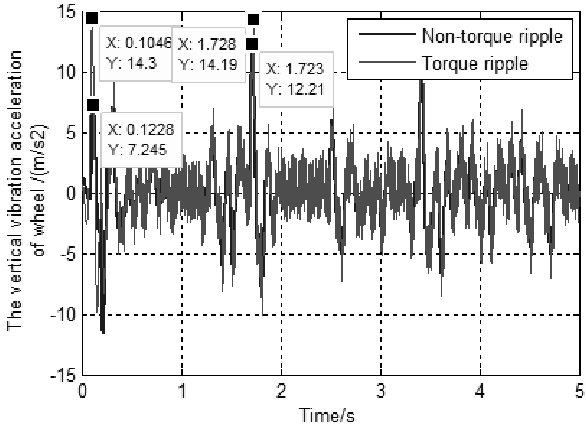

Fig. 11. Response of the vertical vibration acceleration $\ddot{z}_1$ of wheel

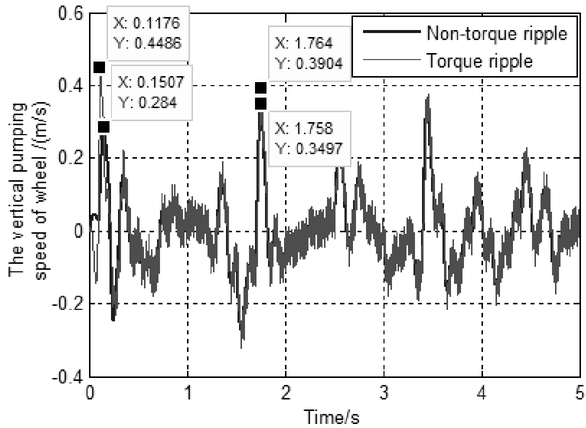

Fig. 12. Response of the vertical vibration acceleration $\ddot{z}_2$ of vehicle

about 4.3 %. It suggests that the torque ripple exerts a small influence on the body of vehicle while a large impact on the wheel, which will reduce the grip of tire.

Figures 11 and 12 respectively show the response curves of the vertical vibration acceleration of wheel and vehicle. It can be observed from the two figures that the growth rate of vertical vibration acceleration is about 49 % around 0.1 s and declines to 14.7 % around 1.7 s as the ripple becomes stable, which indicates a large impact of the torque ripple of motor on the vertical vibration of wheel. Due to the vibration reduction and isolation of suspension, the vertical acceleration of vehicle reaches the peak value around 1.7 s with a low growth rate of 7 %.

Similarly, it can be observed from Figs. 13∼16 that the torque ripple of motor has a large impact on the suspension of vehicle, especially the wheel (unsprung mass).

Conclusions can be drawn from the above analyses that the effect of the torque ripple of in-wheel motor on the vibration of vehicle is quite small while that on the unsprung mass is large which will reduce the grip of tire. That is to way,

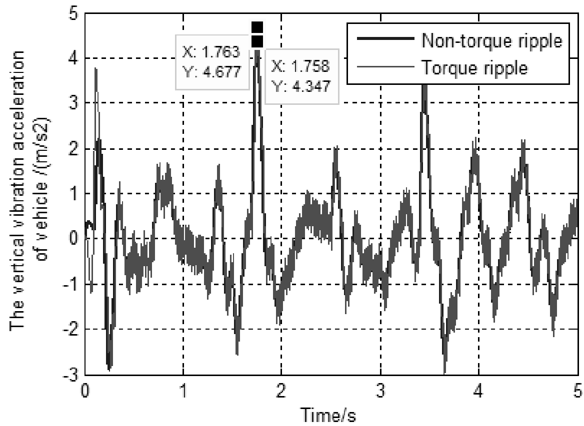

Fig. 13. Response of the vertical pumping speed $\dot{z}_1$ of wheel

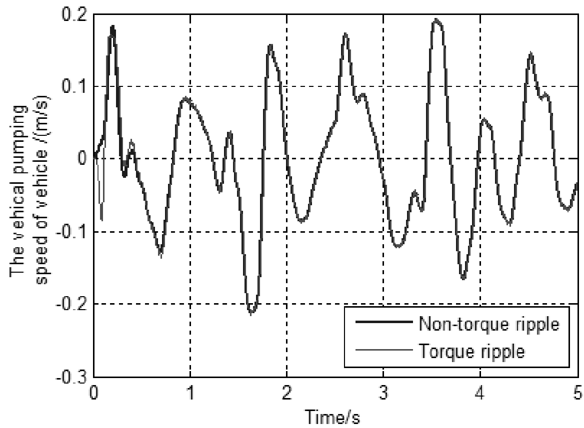

Fig. 14. Response of the vertical pumping speed $\dot{z}_2$ of vehicle

the vehicle riding comfortability is slightly affected while the smooth running of vehicle is greatly influenced. Therefore, before the industrial production of in-wheel motor electric vehicle, effective measures should be taken to improve the suspension structure, optimize parameters, or make innovations in component design. Thus, the running smoothness and power performance of in-wheel-motor electric vehicle can be improved.

7. Conclusion

Conclusions drawn from the abovementioned analyses are as follows:

1. There shows an obvious fluctuation in the speed and torque of motor after the motor is applied with load. As the load rises, the fluctuation quantity of torque and speed will both increase. Thus, the torque ripple of motor is obvious when

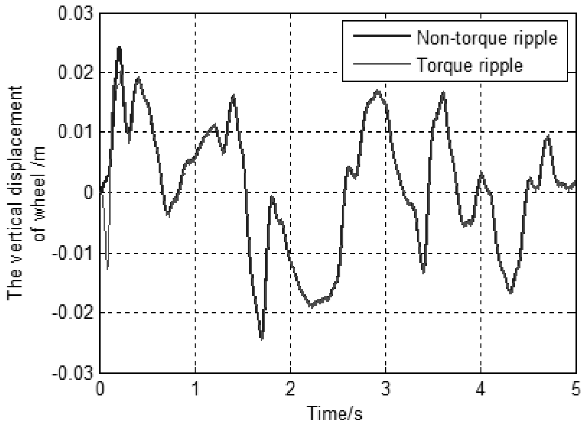

Fig. 15. Response of the vertical displacement z_1 of wheel

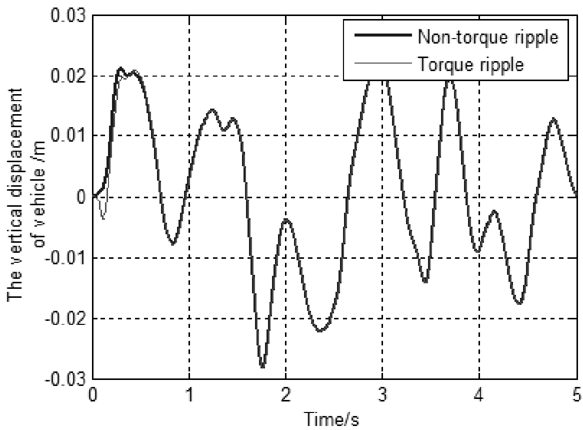

Fig. 16. Response of the vertical displacement z_2 of vehicle

the motor runs with high torque (in which case the vehicle is low in start speed while high in driving speed), which will affect the smooth riding of vehicle as well as reduce the grip of tire.

2. As the in-wheel motor increases the unsprung mass of vehicle, deteriorates the vibration isolation of suspension, and affects the smooth riding of vehicle, further studies should be carried out on the optimization, innovation, and design of the motor vibration system, the torque and speed control of motor, and the design of suspension system so as to mitigate the effect of in-wheel motor on the running performance of vehicle.

3. The ripple of motor torque weakens the gripe of tire. As a result, the vertical vibration of vehicle is intensified and the driving force of vehicle becomes unstable, which is detrimental to the driving system and running safety of vehicle. Thus, it is urgent to carry out further studies on the vertical ki-

netics of in-wheel-motor electric vehicle as well as the suppression method of mechanical-electric coupling vibration.

References

[1] S. Murata: *Vehicle dynamics innovation with in-wheel motor.* SAE Technical Paper 2011-39-7204, 2011.

[2] R. Rojas, A. Niederkofler, J. Willberger: *Comfort and safety enhancement of passenger vehicles with in-wheel motors.* SAE Technical Paper 2010-01-1146, 2010.

[3] D. J. Han, Z. Yan, F. Xiao, S. K. Li: *Development of an advanced stability control system of 4wd electric vehicle with in-wheel-motors.* SAE Technical Paper 2016-01-1671, 2016.

[4] Q. P. Chen, C. J. Liao, A. G. Ouyang, X. Q. Li, Q. A. Xiao: *Research and development of in-wheel motor driving technology for electric vehicles.* International Journal of Electric and Hybrid Vehicles *8*, (2016), No. 3, 242–254.

[5] L. Zhang, L. Li, B. N. Qi, J. Song: *Configuration analysis and performance comparison of drive systems for pure electric vehicle.* SAE Technical Paper 2015-01-1165, 2015.

[6] G. H. Xu, Y. Y. Wang, Y. N. Li, W. Sun: *Analyze for vertical vibration of the in-wheel motor electric vehicle based on power flow method.* Advanced Materials Researchs *915–916* (2014), 444–447.

[7] Y. Zhang, H. Teng, C. Hou: *Research and design of time domain simulation system for vehicle road stochastic irregularity.* Transactions of the Chinese Society of Agricultural Engineering *21* (2005), No. 2, 86–91.

[8] Z. G. Hu, L. P. Chen, Y. L. Zhang, S. Y. Song, W. F. Guo: *Wavelet analysis on nonstationary random road irregularities.* Advanced Materials Research *346* (2011), 689–675.

[9] M. Fasil, C. Antaloae, N. Mijatović, B. B. Jensen, J. Holboll: *Improved dq-axes model of PMSM considering airgap flux harmonics and saturation.* IEEE Transactions on Applied Superconductivity *26* (2016), No. 4, 1–5.

[10] R. S. Rama, P. Latha: *An effective torque ripple reduction for permanent magnet synchronous motor using ant colony optimization.* International Journal of Fuzzy Systems *17* (2015), No. 4, 577–584.

Received October 31, 2017